Linear instability of magnetic Taylor-Couette flow with Hall effect

Günther Rüdiger*
Astrophysikalisches Institut Potsdam, An der Sternwarte 16, D-14482 Potsdam, Germany

Dima Shalybkov†
A.F. Ioffe Institute for Physics and Technology, 194021, St. Petersburg, Russia

(Received 8 May 2003; published 22 January 2004)

The influence of the Hall effect on the linear marginal stability of a molecular hydrodynamic Taylor-Couette flow in the presence of an axial uniform magnetic field is considered. The Hall effect leads to the situation that the Taylor-Couette flow becomes unstable for *any ratio* of the angular velocities of the inner and outer cylinders. The instability, however, does not exist for both signs of the axial magnetic field B_0. For positive shear $d\Omega/dR$ the Hall instability exists for negative Hartmann number and for negative shear $d\Omega/dR$ the Hall instability exists for positive Hartmann number. For negative shear, of course, the Hall instability combines with the magnetorotational instability, resulting in a rather complex bifurcation diagram. In this case the critical magnetic Reynolds numbers with Hall effect are much lower than without Hall effect. In order to verify the presented shear-Hall instability at the laboratory with experiments using liquid metals, one would need rather large magnetic fields ($\sim 10^7$ G).

DOI: 10.1103/PhysRevE.69.016303 PACS number(s): 47.20.Ft, 47.20.−k, 47.65.+a

I. INTRODUCTION

The Taylor-Couette flow between concentric rotating cylinders (Fig. 1) is a classical problem of hydrodynamic and hydromagnetic stability [1,2]. Viscosity included and in the absence of any tangential pressure gradient the most general form of the angular velocity Ω of the flow is

$$\Omega(R) = a + \frac{b}{R^2}, \tag{1}$$

where a and b are two constants related to the angular velocities $\Omega_{\rm in}$ and $\Omega_{\rm out}$ with which the inner and outer cylinders are rotating. With $R_{\rm in}$ and $R_{\rm out}$ ($R_{\rm out} > R_{\rm in}$) being the radii of the two cylinders one finds

$$a = \Omega_{\rm in}\frac{\hat{\mu} - \hat{\eta}^2}{1 - \hat{\eta}^2} \quad \text{and} \quad b = \Omega_{\rm in} R_{\rm in}^2 \frac{1 - \hat{\mu}}{1 - \hat{\eta}^2}, \tag{2}$$

where

$$\hat{\mu} = \Omega_{\rm out}/\Omega_{\rm in} \quad \text{and} \quad \hat{\eta} = R_{\rm in}/R_{\rm out}. \tag{3}$$

According to the Rayleigh criterion the ideal flow is stable whenever the specific angular momentum increases outwards $d(R^2\Omega)^2/dR > 0$ or

$$\hat{\mu} > \hat{\eta}^2. \tag{4}$$

The viscosity, however, has a stabilizing effect so that a flow with $\hat{\mu} < \hat{\eta}^2$ becomes unstable if the Reynolds number of the inner rotation exceeds some critical value.

If it is not too strong, the magnetic field can play a destabilizing role and can lead to magnetorotational instability (MRI). This MRI was discovered decades ago for Taylor-Couette flow [3,4], but its importance as the source of turbulence in accretion disks with differential (Keplerian) rotation was only recognized by Balbus and Hawley [5]. In the molecular hydrodynamic (MHD) regime the Rayleigh criterion for stability, Eq. (4), changes to

$$\hat{\mu} > 1 \tag{5}$$

for a weak magnetic field. The hydrodynamic Taylor-Couette flow is only stable if its angular momentum increases with radius but the hydromagnetic Taylor-Couette flow is stable if the angular velocity itself increases with radius. The MRI decreases the critical Reynolds number for weak magnetic field strengths for hydrodynamically unstable flow and it destabilizes the hydrodynamically stable flow for

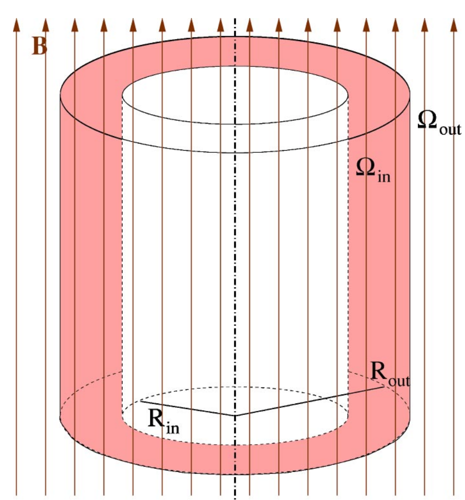

FIG. 1. Cylinder geometry of the Taylor-Couette flow.

*Electronic address: gruediger@aip.de
†Electronic address: dasha.astro@mail.ioffe.ru

$$\hat{\eta}^2 < \hat{\mu} < 1. \tag{6}$$

There are very basic facts for the MRI. At first, MRI depends only on the amplitude of the magnetic field and does not depend on its direction. At second, MRI exists in hydrodynamically unstable situations ($\hat{\mu} < \hat{\eta}^2$) only if the magnetic Prandtl number Pm is not very small as shown in [4] already and later in [6–9]; the critical Reynolds numbers vary as 1/Pm for hydrodynamically stable flows ($\hat{\eta}^2 < \hat{\mu} < 1$) [7,8], so that it is the magnetic Reynolds number which directs the instability. Pm is really very small for laboratory conditions (10^{-5} and smaller). This is the main reason why the MRI has never been observed experimentally in the laboratory.

The importance of the MRI for accretion disk physics and for planned new experiments [6,10,11] highly stimulated the theoretical investigation of the stability of the Taylor-Couette flow [6–12].

Here we are discussing the marginal stability of a fluid with Hall effect. The influence of the Hall effect on MRI was first discussed by Wardle [13] and later by Balbus and Terquem [14] and Sano and Stone [15,16] in relation to accretion physics. We mainly shall consider only axisymmetric disturbances but in relation to the Cowling theorem of dynamo theory also the nonaxisymmetric modes with $m=1$ are concerned.

II. BASIC EQUATIONS

R, ϕ, and z are the cylindric coordinates. A viscous electrically conducting incompressible fluid between two rotating infinite cylinders in the presence of a uniform axial magnetic field admits the basic solution $U_R = U_z = B_R = B_\phi = 0$ and

$$B_z = B_0 = \text{const}, \quad U_\phi = aR + \frac{b}{R}, \tag{7}$$

where $\mathbf{U}$ is the velocity, $\mathbf{B}$ is the magnetic field, and a and b are given by Eqs. (2). We are interested in the stability of this solution. The perturbed state of the flow is described by

$$u'_R,\ R\Omega + u'_\phi,\ u'_z,\ B'_R,\ B'_\phi,\ B_0 + B'_z. \tag{8}$$

The linear stability problem is considered in full generality with nonaxisymmetric perturbations. By developing the disturbances into normal modes, the solutions of the linearized MHD equations are considered in the form

$$u'_R = u_R(R) e^{i(m\phi + kz + \omega t)}, \quad B'_R = B_R(R) e^{i(m\phi + kz + \omega t)},$$

$$u'_\phi = u_\phi(R) e^{i(m\phi + kz + \omega t)}, \quad B'_\phi = B_\phi(R) e^{i(m\phi + kz + \omega t)},$$

$$u'_z = u_z(R) e^{i(m\phi + kz + \omega t)}, \quad B'_z = B_z(R) e^{i(m\phi + kz + \omega t)}. \tag{9}$$

The equations have been derived by Chandrasekhar [17] and Roberts [18]. We use here only a different Ohm's law and different normalizations.

The general form of the induction equation with Hall effect is

$$\frac{\partial \mathbf{B}}{\partial t} = \text{rot}\ (\mathbf{u} \times \mathbf{B}) - \beta\ \text{rot}(\text{rot}\ \mathbf{B} \times \mathbf{B}) + \eta \Delta \mathbf{B}, \tag{10}$$

with η as the magnetic diffusivity and β the Hall parameter which both are considered as uniform in the presented calculations. The electric field for which the induction equation (10) results is

$$\mathbf{E} = \frac{\mathbf{J}}{\sigma} - \mathbf{u} \times \mathbf{B} + \beta(\text{rot}\ \mathbf{B} \times \mathbf{B}). \tag{11}$$

We have used the additional relations div$\mathbf{B}=0$ and $\mathbf{J} = 1/\mu_0$ rot $\mathbf{B}$. The Navier-Stokes equation is used in its standard form, i.e.,

$$\rho\left(\frac{\partial \mathbf{u}}{\partial t} + (\mathbf{u} \cdot \nabla)\mathbf{u}\right) = -\nabla P + \rho \nu \Delta \mathbf{u} + \mathbf{J} \times \mathbf{B}. \tag{12}$$

Let $d = R_{\text{out}} - R_{\text{in}}$ be the gap between the cylinders. We use

$$H = (R_{\text{in}} d)^{1/2} \tag{13}$$

as the unit of length, the velocity η/H as the unit of the perturbed velocity, ν/H^2 as the unit of frequencies, B_0 as the unit of the magnetic field fluctuations, H^{-1} as the unit of the wave number, and Ω_{in} as the unit of the Ω. The dimensionless numbers of the problem are the magnetic Prandtl number

$$\text{Pm} = \frac{\nu}{\eta}, \tag{14}$$

where ν is the kinematic viscosity, Ha is the Hartmann number, and Re is the Reynolds number of the inner rotation:

$$\text{Ha} = \frac{B_0 H}{\sqrt{\mu_0 \rho \nu \eta}}, \quad \text{Re} = \frac{\Omega_{\text{in}} H^2}{\nu}, \tag{15}$$

where ρ is the density. We only consider marginal stability and stationary modes, i.e., $\omega = 0$. Using the same symbols for normalized quantities as before, the equations can be written as a system of ten equations of first order, i.e.,

$$\frac{du_R}{dR} = -\frac{u_R}{R} - i\frac{m}{R}u_\phi - iku_z, \tag{16}$$

$$\frac{du_\phi}{dR} = X_2 - \frac{u_\phi}{R}, \tag{17}$$

$$\frac{du_z}{dR} = X_3, \tag{18}$$

$$\frac{dX_1}{dR} = \left(\frac{m^2}{R^2} + k^2\right)u_R + i(\omega + m\text{Re}\Omega)u_R + 2i\frac{m}{R^2}u_\phi - 2\text{Re}\Omega u_\phi - ik\text{Ha}^2 B_R, \tag{19}$$

$$\frac{dX_2}{dR}=\left(\frac{m^2}{R^2}+k^2\right)u_\phi+i(\omega+m\mathrm{Re}\Omega)u_\phi-2i\frac{m}{R^2}u_R+2a\mathrm{Re}u_R$$
$$-ik\mathrm{Ha}^2B_\phi+\frac{m^2}{R^2}u_\phi+k\frac{m}{R}u_z-i\frac{m}{R}X_1, \tag{20}$$

$$\frac{dX_3}{dR}=\left(\frac{m^2}{R^2}+k^2\right)u_z+i(\omega+m\mathrm{Re}\Omega)u_z-\frac{X_3}{R}-ik\mathrm{Ha}^2B_z$$
$$+k\frac{m}{R}u_\phi+k^2u_z-ikX_1, \tag{21}$$

$$\frac{dB_R}{dR}=-\frac{B_R}{R}-i\frac{m}{R}B_\phi-ikB_z, \tag{22}$$

$$\frac{dB_\phi}{dR}=X_4-\frac{B_\phi}{R}, \tag{23}$$

$$\frac{dB_z}{dR}=i\left(\frac{m^2}{kR^2}+k\right)B_R-\frac{\mathrm{Pm}}{k}(\omega+m\mathrm{Re}\Omega)B_R+u_R-\frac{m}{kR}X_4$$
$$-i\hat{\beta}\frac{m}{R}B_z+i\hat{\beta}kB_\phi, \tag{24}$$

$$\frac{dX_4}{dR}=\left(\frac{m^2}{R^2}+k^2\right)B_\phi+i\mathrm{Pm}(\omega+m\mathrm{Re}\Omega)B_\phi-2i\frac{m}{R^2}B_R$$
$$-iku_\phi+2\mathrm{Pm\,Re}\frac{b}{R^2}B_R+\hat{\beta}\frac{m^2}{R^2}B_R-\hat{\beta}^2\frac{km}{R}B_z$$
$$+\hat{\beta}^2k^2B_\phi+i\hat{\beta}(\omega+m\mathrm{Re}\Omega)\mathrm{Pm}B_R-i\hat{\beta}ku_R$$
$$+i\hat{\beta}\frac{m}{R}X_4, \tag{25}$$

with

$$\hat{\beta}=\frac{\beta B_0}{\eta}. \tag{26}$$

Introducing dimensionless quantities the latter can also be written as

$$\hat{\beta}=\beta_0\mathrm{Pm}^{1/2}\mathrm{Ha}, \tag{27}$$

with

$$\beta_0=\frac{\beta}{R_{\mathrm{out}}}\sqrt{\frac{\mu_0\rho}{\hat{\eta}(1-\hat{\eta})}}. \tag{28}$$

The definitions of X_2, X_3, and X_4 follow from Eqs. (17), (18), and (23) and the X_1 is given by

$$X_1=\frac{du_R}{dR}+\frac{u_R}{R}-P-\mathrm{Ha}^2B_z, \tag{29}$$

with P as the pressure fluctuation. The influence of the Hall effect is indicated by the $\hat{\beta}$ terms in Eqs. (24) and (25). Within the frame of the short-wave approximation, without the induction of the flow field and for small β a local dispersion relation of the form

$$\mathrm{Rm}\propto-\frac{1}{\beta d\Omega/dR} \tag{30}$$

results with magnetic Reynolds number Rm = Pm Re, indicating that positive β and negative shear $d\Omega/dR$ form the same instability as negative β and positive shear $d\Omega/dR$.

An appropriate set of ten boundary conditions is needed to solve the system (16)–(25). It is easy to see that the Hall effect leaves the boundary conditions used in [8] as unchanged, i.e., the no-slip conditions for the velocity,

$$u_R=u_\phi=u_z=0, \tag{31}$$

and for the magnetic field,

$$\frac{dB_\phi}{dR}+\frac{B_\phi}{R}=0,\quad B_R=0, \tag{32}$$

for conducting walls. The boundary conditions are valid for $R=R_{\mathrm{in}}$ and for $R=R_{\mathrm{out}}$. For insulating walls the magnetic boundary conditions are different at $R=R_{\mathrm{in}}$ and $R=R_{\mathrm{out}}$, i.e.,

$$B_R+i\frac{B_z}{I_m(kR)}\left(\frac{m}{kR}I_m(kR)+I_{m+1}(kR)\right)=0 \tag{33}$$

for $R=R_{\mathrm{in}}$ and

$$B_R+i\frac{B_z}{K_m(kR)}\left(\frac{m}{kR}K_m(kR)-K_{m+1}(kR)\right)=0 \tag{34}$$

for $R=R_{\mathrm{out}}$ where I_n and K_n are the modified Bessel functions. With

$$B_\phi-\frac{m}{kR}B_z=0, \tag{35}$$

the condition for the toroidal field is the same at both locations.

III. RESULTS

The numerical method is already described in our papers [7] and [8]. Here only the results including the Hall effect are presented.

A. Positive shear

In the present section an instability is described which exists only in the presence of the Hall effect. It destabilizes flows with $\hat{\mu}>1$ (i.e., with positive shear $d\Omega/dR$) for which so far no other instability is known. Figures 2–4 illustrate the instability for both conducting and nonconducting boundary conditions for a container with a wide gap ($\hat{\eta}=0.5$). The flow is unstable but only for negative Hartmann number, i.e., if angular velocity and magnetic field have opposite directions. The result depends on the sign of the Hall resistiv-

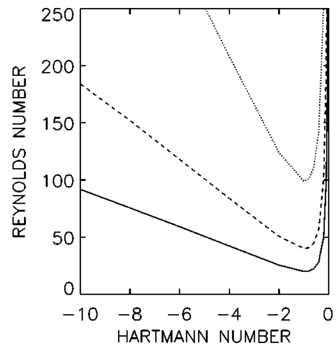

FIG. 2. The line of marginal stability for magnetic Taylor-Couette flow with Hall effect ($\beta_0=1$) for $\hat{\eta}=0.5$, $\mathrm{Pm}=1$ and for positive $d\Omega/dR$: $\hat{\mu}=2$ (solid line), 1.5 (dashed line), and 1.2 (dotted line). Boundary conditions (32) for *conducting* cylinder walls.

ity; here the positive Hall resistivity is used. For negative Hall resistivity the orientation is opposite. The fact that Hall effect destabilizes flows with the angular velocity increasing outwards was already described by Balbus and Terquem [14].

For small Hartmann number the β^{-1} behavior of Eq. (30) is confirmed and for strong magnetic fields the instability is suppressed. The minimum value of the Reynolds number already results for Hartmann number of order unity; it becomes smaller and smaller for increasing shear [see the estimate (30)]. Figure 4 demonstrates the validity of the relation $\mathrm{Re}\propto 1/\mathrm{Pm}$ which is also indicated by the relation (30). Again the Reynolds number takes its minima at such Hartmann numbers that the Lundquist number $\mathrm{Ha}^*=\mathrm{Ha}\sqrt{\mathrm{Pm}}$ is constant.

Figures 2 and 3 demonstrate that the influence of the boundary conditions is not negligible what is quite characteristic for the magnetic Taylor-Couette problem (even in the small-gap approximation) as shown already by Niblett [19] and later by Rüdiger *et al.* [8]. In particular, for vacuum boundary conditions the suppression of the instability by strong magnetic fields is a rather weak effect compared with the magnetic suppression in a container with perfect-conducting cylinder walls. Once the Reynolds number exceeds the minimum value given in the Fig. 3, then the Taylor-Couette flow is unstable for a very wide range of Hartmann numbers.

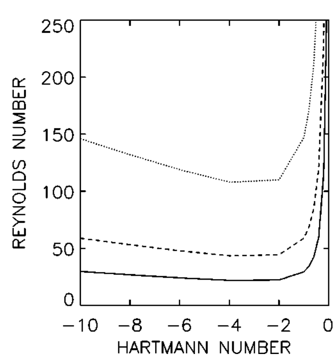

FIG. 3. The same as in Fig. 2 but for the *vacuum* boundary conditions (33)–(35). Note the very weak influence of the magnetic field on the onset of the instability.

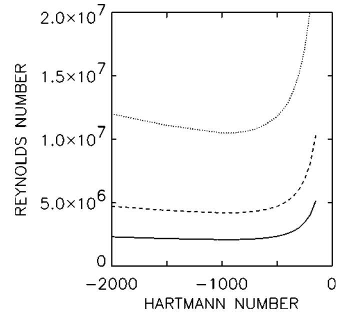

FIG. 4. The same as in Fig. 3 but for $\mathrm{Pm}=10^{-5}$.

According to Eq. (2), the rotation law does not depend on the inner angular velocity Ω_{in} for $\hat{\mu}\gg 1$ and the situation is practically the same as if the inner cylinder were at rest. In this case, the Reynolds number of the outer rotation, $\mathrm{Re}_{\mathrm{out}}$, is the real parameter of the problem instead of Re:

$$\mathrm{Re}_{\mathrm{out}}=\hat{\mu}\mathrm{Re}=\frac{\Omega_{\mathrm{out}}H^2}{\nu}. \tag{36}$$

We have indeed numerically confirmed a behavior such as $\mathrm{Re}\propto 1/\hat{\mu}$ for large $\hat{\mu}$. The value of $\mathrm{Re}_{\mathrm{out}}$ corresponding to minimal Re (which is for Hartmann number of order unity) is

$$\mathrm{Re}\simeq 20. \tag{37}$$

In Fig. 5 the critical wave numbers are given for which the Reynolds number is minimum for given Hartmann number. The three curves represent the solutions with different boundary conditions. The solid line stands for vacuum conditions for both cylinders while the dashed line concerns perfect-conductor solutions. If the outer boundary condition concerns the vacuum and if within the inner cylinder there is a perfect conductor, then the dot-dashed line gives the wave numbers. As expected, the standard behavior can be observed; i.e., the wave number sinks for growing magnetic field so that the cells are elongated parallel to the magnetic field lines. The vertical extension of one cell follows from the relation

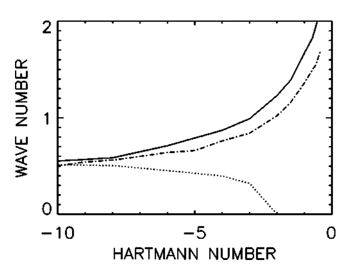

FIG. 5. The dependence of the critical wave numbers on the magnetic field for various boundary conditions: vacuum conditions (solid lines), perfect-conductor conditions (dashed lines), and mixed conditions (vacuum outer cylinder, perfect conductor inner cylinder, dot-dashed lines). $\hat{\mu}=2$.

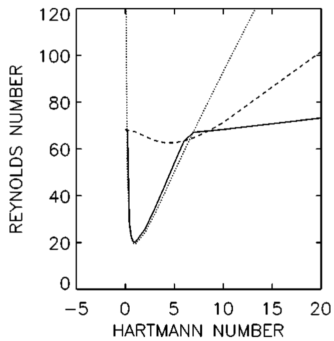

FIG. 6. The same as in Fig. 2 but for resting outer cylinder ($\hat{\mu}=0$, i.e., negative $d\Omega/dR$). $\beta_0=0$ (dashed line) and $\beta_0=1$ (solid line). The dotted line is for $\beta_0=1$, but for $\mathbf{u}=0$ (velocity fluctuations neglected, i.e., kinematic case). The minimum of the dashed line indicates the Lorentz force-induced MRI.

$$\frac{\delta z}{R_{\rm out}-R_{\rm in}}=\frac{\pi}{k_{\rm crit}} \tag{38}$$

(for $\hat{\eta}=0.5$). For perfect-conducting cylinders, however, the trend is opposite. For this case the vertical wave number $k_{\rm crit}$ becomes very small for small Hartmann numbers. The reason is that a solution $B_\phi \propto R^{-1}$ and $B_R=0$ exists which fulfills the boundary conditions (32) and Eqs. (16)–(25) for $\omega=k=\mathrm{Ha}=0$. This current-free solution, however, is always marginal so that it cannot be excited if it does not exist at the beginning. If one of the boundary conditions differs from Eq. (32), then this solution cannot exist and the wave numbers have their normal behavior as shown in Fig. 5.

B. Negative shear

The Hall effect also modifies the critical Reynolds numbers for both hydrodynamically unstable flows ($\hat{\mu}<\hat{\eta}^2$) and for magnetohydrodynamically unstable flow ($\hat{\mu}<1$) resulting in a rather complex situation illustrated with Fig. 6. The dashed line is the MRI without Hall effect and the dotted line is the shear-Hall instability with neglected flow perturbations, i.e., without MRI. It is insofar the counterpart to the lines in Fig. 2. An instability is shown of the axial magnetic field as the result of a combination of shear and Hall effect. The combination of MRI and this shear-Hall instability is given as the solid line in Fig. 6. A deep minimum of the Reynolds number is produced for weak magnetic fields,much deeper than the minimum resulting without Hall effect. On the other hand, for increasing Hartmann numbers the solid line has a very weak slope so that the magnetic-field dependence of the combined instability ('HMRI') is rather weak as already shown by Wardle ([13]; see his Fig. 1c). Again the Hall effect is important for only one orientation of the magnetic field.

IV. NONAXISYMMETRIC MODES

It is also important to probe the existence of nonaxisymmetric modes. After the Cowling theorem only nonaxisymmetric modes can be maintained by a dynamo process. We

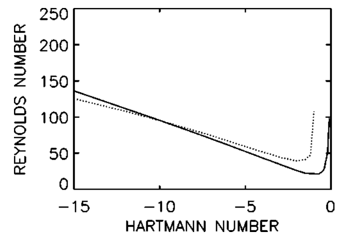

FIG. 7. The lines of marginal instability for conducting cylinder walls for $\hat{\mu}=2$ with axisymmetric ($m=0$, solid line) and nonaxisymmetric ($m=1$, dotted line) modes. Note the crossover of both lines.

already have discussed the appearance of nonaxisymmetric modes for the magnetic Taylor-Couette flow with negative shear. The common result was that the lines of marginal stability for $m=0$ and $m=1$ have a very different behavior for different electrical boundary conditions [12]. One finds crossovers of the stability lines for $m=0$ and $m=1$ for containers with conducting cylinder walls and one never finds such crossovers for containers with vacuum boundary conditions. The same happens here for the shear-Hall instability for magnetic Taylor-Couette flows with positive shear, i.e., $\hat{\mu}>1$. In Fig. 7 the lines for both axisymmetric and nonaxisymmetric modes are given for conducting boundary conditions and in Fig. 8 they are given for vacuum boundary conditions. The crossover of the lines only exists for conducting cylinder walls. As usual, in the minimum the $m=0$ mode dominates but for stronger magnetic fields the mode with $m=1$ dominates.

V. DISCUSSION

We have shown that the Hall effect destabilizes the magnetic Taylor-Couette flow so that for any value of the parameter $\hat{\mu}$ a critical amplitude and one of the directions of the magnetic field exist for which the flow is unstable.

Taylor-Couette flows with $\hat{\mu}>1$, i.e., with positive shear $d\Omega/dR$, are stable in both hydrodynamic and traditional MRI regimes. If, however, the Hall effect is included in the induction equation, then even such a flow becomes unstable under the influence of an axial magnetic field but only for one of the two possible orientations of the field. For vacuum boundary conditions and not too small magnetic fields there is only a rather weak dependence of the critical Reynolds number on the Hartmann number (see Fig. 3).

The other magnetic orientation destabilizes all the flows

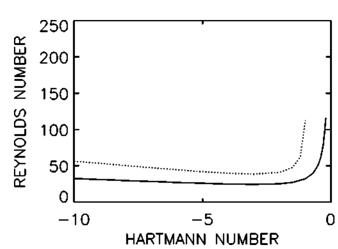

FIG. 8. The same as in Fig. 7 but for vacuum boundary conditions. No crossover of both the lines exist.

TABLE I. Astrophysical objects [protoplanetary disks, pulsars (NS), and white dwarfs (WD)]: Hall coefficient $\mu_0\beta$, magnetic diffusivity, critical magnetic field after Eq. (41), and observed magnetic field.

Object	Hall coeff. (m^3/C)	η (m^2/s)	B_0 (G)	B_{obs} (G)
WD	10^{-20}	10^{-9}	10^9	10^7
NS env.	10^{-25}	10^{-13}	10^{10}	10^{12}
NS core	10^{-28}	10^{-14}	10^{12}	

with $\hat{\mu}<1$, i.e., with negative $d\Omega/dR$ (see Fig. 6). The linearized induction equation (10) is invariant against the transformation

$$B_0 \to -B_0, \quad u_0 \to -u_0, \tag{39}$$

so that the simultaneous change of the signs of $d\Omega/dR$ and B_0 leads to the same instability. After the splitting of the induction equation into poloidal and toroidal components one finds the scheme

$$B_{\rm tor} \xrightarrow[\rm Hall]{} B'_{\rm pol} \xrightarrow[\rm Hall]{\rm shear} B'_{\rm tor}; \tag{40}$$

hence also the shear must be changed if the Hall effect is changed. If this is true, then the shear is necessary for the existence of an instability. The shear appears as the energy source of the instability.

The magnetic field for an important influence of the Hall effect should be very high. The minimum value of the Reynolds number for both positive and negative shear exists for $\hat{\beta}\sim 1$. The corresponding value of the magnetic field is

$$B_0 \simeq \frac{\eta}{\beta}. \tag{41}$$

The Hall coefficient ($\mu_0\beta$ in our notation) for liquid metals is about 10^{-10} m^3/C, with $\eta\sim 10^{-1}$ m^2/s and with $\mu_0 = 4\pi\times 10^{-7}$ for the magnetic field $B_0\simeq 10^7$ G is yielded. This value is too high for the laboratory experiments.

We have another situation for astrophysical applications [13–16]. In Table I the Hall coefficients and the magnetic diffusivities are given for various objects which are so cool or have so huge magnetic fields B_{obs} that the Hall effect is suspected to be important.

The situation in protoplanetary accretion disks is presented in Fig. 9 where the numbers are taken from a model

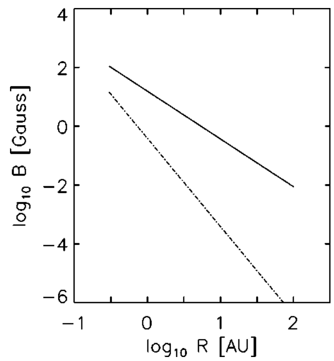

FIG. 9. The magnetic constellation in accretion disks after Sano and Stone [15]. Solid line: magnetic-field amplitude if magnetic Mach number equals unity. Dashed line: magnetic-field amplitude if Hall time scale equals magnetic dissipation decay time.

by Sano and Stone [15]. The amplitude of the magnetic field comes from the condition that the magnetic Mach number equal 1. Above the lowest line the Hall effect dominates the Ohmic dissipation and v.v. One finds that indeed the magnetic field may be so strong that the Hall effect dominates the Ohmic dissipation. The critical magnetic field amplitude at $R=1$ AU is about 0.1 G. Such high values can hardly be imagined as due to a magnetized central object. Polar field strengths of order $\sim 10^5$ G at the surface of a protosun are needed in order to produce 0.1 G at a distance of 1 AU.

Magnetic fields with amplitudes of 1 G at 1 AU should thus only be generated by the action of a (turbulent) dynamo. In this case, however, we cannot use the molecular conductivities to estimate the values of the parameters as it was done in [13–16]. E.g., the turbulent magnetic diffusivity may increase by several orders of magnitude. No considerations of the effect of turbulence on the Hall diffusivity are known to us. This effect might be smaller than the influence on the magnetic diffusivity due to the linear dependence of the Hall diffusivity on the magnetic field. If it is so, then the role of the Hall effect for the weakly ionized protostellar accretion disks might easily be overestimated.

ACKNOWLEDGMENTS

The Deutsche Forschungsgemeinschaft is cordially acknowledged for financial support (Grant No. 436 RUS 113/559). One of the authors (D.S.) also acknowledges financial support by the RFBR (Grant No. 03-02-17522).

[1] M. Couette, Ann. Chim. Phys. **21**, 433 (1890).
[2] G.I. Taylor, Philos. Trans. R. Soc. London, Ser. A **233**, 289 (1923).
[3] E.P. Velikhov, Sov. Phys. JETP **9**, 995 (1959).
[4] U. Kurzweg, J. Fluid Mech. **17**, 52 (1963).
[5] S.A. Balbus and J.F. Hawley, Astrophys. J. **376**, 214 (1991).
[6] H. Ji, J. Goodman, and A. Kageyama, Mon. Not. R. Astron. Soc. **325**, 1 (2001).
[7] G. Rüdiger and D. Shalybkov, Phys. Rev. E **66**, 016307 (2002).
[8] G. Rüdiger, M. Schultz, and D. Shalybkov, Phys. Rev. E **67**, 046312 (2003).
[9] A.P. Willis and C.F. Barenghi, Astron. Astrophys. **388**, 688 (2002).
[10] J. Goodman and H. Ji, J. Fluid Mech. **462**, 365 (2002).
[11] K. Noguchi, H.F. Beckley, and J. Nordhaus, Astrophys. J. **575**,

1151 (2002).

[12] D. Shalybkov, G. Rüdiger, and M. Schultz, Astron. Astrophys. **395**, 339 (2002).

[13] M. Wardle, Astrophys. J. **307**, 849 (1999).

[14] S.A. Balbus and C. Terquem, Astrophys. J. **552**, 235 (2001).

[15] T. Sano and J.M. Stone, Astrophys. J. **570**, 314 (2002).

[16] T. Sano and J.M. Stone, Astrophys. J. **577**, 534 (2002).

[17] S. Chandrasekhar, *Hydrodynamic and Hydromagnetic Stability* (Clarendon, Oxford 1961).

[18] P.H. Roberts, Proc. Cambridge Philos. Soc. **60**, 635 (1964).

[19] E.R. Niblett, Can. J. Phys. **36**, 1509 (1958).